Bioelectrochemistry 140 (2021) 107803

Contents lists available at ScienceDirect

Bioelectrochemistry

journal homepage: www.elsevier.com/locate/bioelechem

Gene transfer by electroporation with high frequency bipolar pulses *in vitro*

Tjaša Potočnik, Damijan Miklavčič, Alenka Maček Lebar *

University of Ljubljana, Faculty of Electrical Engineering, Tržaška 25, 1000 Ljubljana, Slovenia

ARTICLE INFO

Article history:
Received 27 November 2020
Received in revised form 16 March 2021
Accepted 17 March 2021
Available online 22 March 2021

Keywords:
Gene electrotransfer
Electroporation
High frequency pulses
Bipolar pulses

ABSTRACT

High-frequency bipolar pulses (HF-BP) have been demonstrated to be efficient for membrane permeabilization and irreversible electroporation. Since membrane permeabilization has been achieved using HF-BP pulses we hypothesized that with these pulses we can also achieve successful gene electrotransfer (GET). Three variations of bursts of 2 μs bipolar pulses with 2 μs interphase delay were applied in HF-BP protocols. We compared transfection efficiency of monopolar micro and millisecond pulses and HF-BP protocols at various plasmid DNA (pDNA) concentrations on CHO – K1 cells. GET efficiency increased with increasing pDNA concentration. Overall GET obtained by HF-BP pulse protocols was comparable to overall GET obtained by longer monopolar pulse protocols. Our results, however, suggest that although we were able to achieve similar percent of transfected cells, the number of pDNA copies that were successfully transferred into cells seemed to be higher when longer monopolar pulses were used. Interestingly, we did not observe any direct correlation between fluorescence intensity of pDNA aggregates formed on cell membrane and transfection efficiency. The results of our study confirmed that we can achieve successful GET with bipolar microsecond i. e. HF-BP pulses, although at the expense of higher pDNA concentrations.

1. Introduction

When cells are exposed to external electric field of sufficient amplitude and duration transient destabilization of cell membrane is achieved [1,2]. This is called electroporation (also electropermeabilization) and is one of the universal methods used for introducing various molecules into cells *in vitro* and *in vivo*. The most commonly established theory states that during electroporation pores are formed on the cell membrane which allow ions and molecules to enter and/or leave the cell [2,3]. Electroporation is used in medicine [4,5], biotechnology [6] and in food [7] and biomass processing [8].

In medicine electroporation can be used as electrochemotherapy (ECT) for delivery of chemotherapeutic drugs [9,10], irreversible electroporation (IRE) for tissue ablation [11–15], administration of active substances into and through the skin [16,17] or for efficient delivery of DNA into cells and tissues as a method named gene electrotransfer (GET) [18,19]. Among the most promising GET applications in medicine are DNA vaccination and gene therapy. GET enables improved expression of therapeutic or immunogenic proteins that are encoded by DNA or RNA which can be used for the prevention or treatment of many cancers, cardiovascular diseases, autoimmune diseases, organ specific disorders as well as infectious diseases [20–25].

GET is successful only if plasmid DNA (pDNA) is added before the application of the electric pulses [18,26], which according to current knowledge have a dual role in GET; they enable permeabilization of the cell membrane and cause electrophoresis of pDNA that brings pDNA in contact with the cell membrane. During electric field delivery heterogenous population of permeable sites is formed on cell membrane, with longer pulses leading to formation of larger permeable sites [27,28]. Negatively charged pDNA molecules in electric field move due to electrophoretic force and make contact with cell membrane in a larger number compared to free diffusion [29]. If permeable sites on cell membrane are large enough small DNA molecules (equal or smaller than 15 bp [30]) can enter the cell with electrophoresis. Large pDNA molecules form aggregates on cell membrane during electric pulses delivery and after electropermeabilization enter the cell via endocytosis [18,31–33]. Because electrophoresis is involved in pDNA aggregates formation on cell membrane during electric field delivery, the lack of electrophoresis is an important if not essential barrier for use of short pulses in GET *in vitro* and *in vivo* [29,34–36]. However, it was published before, that under optimized conditions the

* Corresponding author at: University of Ljubljana, Faculty of Electrical Engineering, Tržaška 25, 1000 Ljubljana, Slovenia.
E-mail address: alenka.maceklebar@fe.uni-lj.si (A. Maček Lebar).

https://doi.org/10.1016/j.bioelechem.2021.107803
1567-5394/

transfection efficiency with 5 × 400 μs bipolar square wave pulses is better than with the same number of unipolar square wave pulses of same duration or single square pulse of the same cumulative duration [37]. The explanation is offered in symmetric permeabilization of cell membrane and formation of pDNA aggregates on both sides of the cell membrane facing the electrodes not only on one side as with monopolar pulses [29,38] which could lead to an increase in GET efficiency. The lack of electrophoretic force during delivery of short pulses can be partially compensated with higher pDNA concentration which enables that more pDNA molecules are near cell membrane [39]. But increasing pDNA concentration above 100 μg/ml *in vitro* presumably leads to pDNA entanglement which reduces the mobility of pDNA molecules, especially if they are larger than 6 kbp, probably resulting in lower GET efficiency [40].

Electroporation applications are accompanied by some undesirable effects like electrode oxidation, changes in pH and Joule heating [41–45]. While in applications *in vitro* these effects are not considered critical, they are much more relevant in applications *in vivo* and in food industry. Intense pH changes close to the electrodes [46] can be damaging to the cells and tissues and can result in changes in molecules, especially denaturation of pDNA in GET [43,46,47]. The time in which the pH changes between electrodes are neutralized after electroporation based treatments is short in ECT and IRE and much longer in GET [47] due to different pulse parameters used. For ECT and IRE usually shorter pulses with higher voltage are applied, while in GET, longer pulses of lower voltage are used [48].

Recently, the use of short bipolar electroporation pulses applied in bursts with repetition frequencies over 100 kHz, high-frequency bipolar pulses (HF-BP), was proposed [49]. In HF-BP long (100 μs–5 ms) monopolar pulses are replaced with burst of short (0.25–5 μs) bipolar pulses [50,51]. It was shown that with the use of HF-BP pulses similar levels of cell membrane permeabilization *in vitro* [52–54] can be achieved compared to long monopolar pulses which are dominant in current IRE, ECT and GET protocols. *In vivo* experiments have shown that HF-BP pulses are effective in ECT, IRE of tumors and in cardiac ablation [12–14,55–57]. HF-BP pulses are also suggested to provide more uniform distribution of electric field in inhomogeneous tissue, which results in more predictable cellular response and potentially leading to improved clinical precision of IRE, ECT and GET [49,58]. During HF-BP pulses delivery smaller amounts of metal ions are released from electrodes and electrochemical reactions are reduced [41,59]. However, in HF-BP higher electric fields are needed to achieve the same results as with longer monopolar pulses [52,60]. This can lead to increased Joule heating and consequently, thermal damage in the area around the electrodes [42,61]. Also, attention should be given to demonstration of cancelation effect originally observed in sub-microsecond pulses but recently also in range of microsecond pulses where the opposite polarity phase of the pulse cancels the effect of the first phase if the interphase delay is short enough, which might be one of the reasons for lower efficiency [53,59,62,63].

Muscle contractions that cause discomfort and electrical stimulation of sensory nerves [64–67] causing pain are the main disadvantages that accompany the electroporation based treatments with long monopolar pulses and dictates the use of muscle relaxants and anesthesia. Electric pulses delivery, if applied close or in the heart, must also be synchronized with electrocardiogram [68–73]. But the use of HF-BP pulses promises to mitigate muscle contractions and reduce pain during electroporation based treatments [67]. Namely, electrical stimulation studies proved that short bipolar pulses require higher amplitudes for stimulation of nerves and muscles compared to longer pulses [51,67,74,75] and bipolar pulses with long (80–100 μs) interphase delay further increase excitation thresholds [76].

Since membrane permeabilization is a prerequisite for successful GET [18,39] we hypothesize that with HF-BP pulse parameters successful GET can be achieved. HF-BP pulse parameters, used in our experiments, were determined according to previously published experimental and theoretical findings [49,77]. According to previous studies cancellation effect is considerable when delivering 1 μs HF-BP pulses of 1 μs interphase delay [53], while muscle contractions were observed at HF-BP pulses of 5 μs duration and longer [51]. Based on this we chose 2 μs as a duration of positive and negative phase of biphasic pulse and 2 μs interphase delay ensured complete charging and discharging of cell membrane in high-conductivity cell growth medium [53]. The same pulse waveform was shown to substantially decrease the intensity of muscle contractions compared with traditional monopolar pulses [49,50,77]. Because approximately 1 s was reported to be necessary for stable pDNA aggregates formation [29], we chose 1 Hz repetition frequency of bursts.

We first tested the number of pulses in each burst and the number of bursts in accordance with pulse protocols used in [49,77] and then adjusted them to achieve considerable GET efficiency with minimal effect on cell viability. Transfection efficiency obtained by HF-BP protocols at various pDNA concentrations was compared to that of "classical", monopolar micro (8 × 100 μs) and millisecond (8 × 5 ms) pulses.

2. Materials and methods

2.1. Cells

We used Chinese hamster ovary cell line (CHO-K1; European Collection of Cell Cultures, Great Britain). Cells were grown in 25 mm^2 culture flasks (TPP, Switzerland) for 2–4 days in an incubator (Kambič, Slovenia) at 37 °C, in a humidified atmosphere of 5% CO_2 in air. CHO cells were cultured in HAM-F12 growth medium (PAA, Austria) supplemented with 10% fetal bovine serum (Sigma Aldrich, Germany), L-glutamine (StemCell, Canada) and antibiotics penicillin/streptomycin (PAA, Austria), and gentamycin (Sigma Aldrich, Germany).

For experiments cells in exponential growth phase were trypsinized using trypsin – EDTA; 5 g trypsin/2 g EDTA in 0.9% NaCl (Sigma Aldrich, Germany) 10 × diluted in Hanks' Balanced Salt solution (Sigma Aldrich, Germany). From the obtained cell suspension, trypsin and growth medium were removed by centrifugation at 180 g for 5 min at room temperature (Sigma 3–15 K, UK). The cell pellet was then resuspendend in HAM-F12 growth medium to obtain a final cell density of 6.6 × 10^5 cells/ml.

2.2. Plasmid

A 4.7 kb plasmid pEGFP-N1 (Clontech Laboratories Inc., USA) encoding green fluorescent protein (GFP) under the control of CMV promotor was used. Plasmid (pDNA) was amplified using Escherichia coli and isolated with HiSpeed Plasmid Maxi Kit (Qiagen, Germany). pDNA concentration was spectrophotometrically determined at 260 nm. We tested seven pDNA concentrations, namely 20, 40, 60, 80, 100, 250 and 500 μg/ml.

2.3. Electric pulses

Five different pulse protocols were used in our experiments, namely 8 × 100 μs: 8 pulses, 100 μs duration, 1 Hz repetition frequency; 8 × 5 ms: 8 pulses, 5 ms duration, 1 Hz repetition frequency and three HF-BP pulse protocols. In HF-BP pulse protocols bipolar pulses of 2 μs duration of positive and negative phase were applied. The pause between positive and negative

pulse phase and pause between bipolar pulses in all three pulse protocols were 2 μs. Number of pulses in each burst and number of bursts were varied, while burst repetition frequency was 1 Hz in all three HF-BP protocols. Pulse protocol HF-BP 1 consisted of 20 bursts and in each burst 216 pulses were applied. Pulse protocol HF-BP 2 consisted of 50 bursts; in each burst 50 pulses were applied. And pulse protocol HF-BP 3 consisted of 100 bursts; in each burst 32 pulses were applied. Electric field was estimated as the voltage applied divided by the distance between the electrodes. For all pulse protocols the range 0–2 kV/cm was tested for cell membrane permeabilization and cell viability. For each pulse protocol we determined GET efficiency on the interval of electric fields below and above the intersection of permeabilization and cell viability curves. Based on these results we decided on electric field used in our GET experiments. Pulse parameters of all five pulse protocols used in GET experiments are summarized in Tables 1 and 2 and Supplementary schematic 1.

For the application of pulses, a laboratory prototype pulse generator (University of Ljubljana) based on H-bridge digital amplifier with 1 kV MOSFETs (DE275-102N06A, IXYS, USA) was used [52]. During each experiment voltage and current applied to sample were measured with differential probe (ADP305, LeCroy, USA) and current probe (CP030, LeCroy, USA) and monitored on oscilloscope (Wavesurfer 422, 200 MHz, LeCroy, USA). Representative measurements of voltage and current in HF-BP pulse protocols are shown in Supplementary Fig. 1.

2.4. Permeabilization

For permeabilization detection 150 μl of cell suspension ($1x10^5$ cells) with 5 μl of propidium iodide, final concentration 33 μg/ml, (Life Technologies, USA) was pipetted into 4 mm cuvettes (VWR International, Belgium). After pulse application cells were incubated for 10 min at room temperature. Propidium iodide incorporation into cells was detected with flow cytometer (Attune® NxT, Life Technologies, USA) using a blue laser excitation at 488 nm and detecting the emitted fluorescence through a 574/26 nm band-pass filter. At every measurement 10,000 events were recorded. Data obtained were analyzed with the Attune NxT software. The voltage that was applied to the cuvette was varied in the 100–800 V range, corresponding to 0.25–2 kV/cm electric field.

2.5. Gene electrotransfer

150 μl of cell suspension ($2x10^5$ cells) were pipetted into 4 mm cuvette and various concentrations of pDNA were added. We tested final concentrations of 20, 40, 60, 80, 100, 250 or 500 μg/ml pDNA in cell suspension. Cells were incubated with pDNA for 2 min at room temperature then electric pulses were applied as described above. To increase cell viability 37.5 μl (25% of volume) of fetal bovine serum (Sigma Aldrich, Germany) was added immediately after pulse delivery and cells were incubated in cuvette for 5 min at 37 °C in a humidified atmosphere in a 5% CO_2 incubator [78,79]. After incubation cell suspension was transferred to 1 ml of HAM-F12 growth medium in 24 well plate (TPP, Switzerland) and incubated for 24 h at 37 °C in a humidified atmosphere in a 5% CO_2 incubator. Afterwards, cells were trypsinized as described above and percent of GFP positive cells and median fluorescence of GFP positive cells were detected using flow cytometer (Attune® NxT, USA). Excitation wavelength was detected with a blue laser at 488 nm and emitted fluorescence was through a 530/30 nm band-pass filter. At every measurement 10,000 events were recorded. Obtained data were analyzed with the Attune NxT software.

2.6. Cell viability

After cells were exposed to pulse protocols at different electric fields (cell viability curve) or pulse protocols at fixed electric field with different pDNA concentrations (cell viability after GET) $2x10^4$ cells were transferred to HAM-F12 growth medium prepared previously in wells of 96-well plate (TPP, Switzerland). Three samples were taken from each cuvette. Cells were placed in the incubator (37 °C, 5% CO_2) for 24 h. Cell viability was determined with the MTS-based Cell Titer 96 AQueous One Solution Cell Proliferation Assay (Promega, USA). After 24 h incubation 20 μl of MTS reagent were added to each well and cells were incubated for additional 2 h in the incubator (37 °C, 5% CO_2). Absorption at 490 nm wavelength was measured with a Tecan Infinite M200 spectrophotometer (Tecan, Switzerland). An average absorption obtained in the samples containing only growth medium was subtracted from the absorption measured in cell samples. To calculate the percentage of viable cells the absorption of each sample was divided by an average absorption of the control samples.

2.7. Visualization of pDNA interaction with cell membrane

To visualize pDNA interaction with cell membrane TOTO-1 (Molecular Probes — Invitrogen, USA) nucleic acid stain was used. The protocol of staining was the same as in [80,81]. Briefly, the plasmid pEGFP-N1 was labeled with 2.3×10^{-4} M TOTO-1 DNA intercalating dye with an average base pair to dye ratio of 5 for 60 min on ice and in the dark.

1×10^5 CHO cells were plated as a monolayer culture in Lab-Tek chambered coverglass (Nunc, TermoFisher Scientifc, USA) for 8 h in cell growth medium at 37 °C in a humidified 5% CO_2 atmosphere in the incubator. Immediately before electric pulse application, growth medium was removed and fresh growth medium with labeled pDNA was added to cells in 20 μg/ml or 500 μg/ml concentration. A pair of two parallel Pt/Ir wire electrodes, with 4 mm distance between inner edges, was positioned to the bottom of Lab-Tek chamber and samples were exposed to electric pulses. Only HF-BP 2, 8 × 100 μs and 8 × 5 ms protocols were tested.

To monitor the interaction of pDNA with the cell membrane fluorescent microscope (Zeiss 200, Axiovert, Germany) was used with 100 × oil immersion objective. The images were recorded using imaging system (MetaMorph imaging system, Visitron, Germany). Fluorescence emission along the cell membrane was analyzed (MetaMorph, Germany) and the fluoresce intensity along perime-

Table 1
Pulse parameters of all pulse protocols.

Protocol	Duration of positive phase (μs)	Duration of negative phase (μs)	Pause between positive and negative phase (μs)	Pause between pulses (μs)	Number of pulses in each burst	Number of bursts	Burst repetition frequency (Hz)	Electric field (kV/cm)
8 × 100 μs	100	0	0	0	1	8	1	1.6
8 × 5 ms	5000	0	0	0	1	8	1	0.5
HF-BP 1	2	2	2	2	216	20	1	1
HF-BP 2	2	2	2	2	50	50	1	1.25
HF-BP 3	2	2	2	2	32	100	1	1.25

Table 2
Cumulative parameters of all pulse protocols. Dose = voltage^2 × On-time per burst was calculated according to [77].

Protocol	On time per pulse (μs)	On-Time per Burst (μs)	On-Time per treatment (μs)	Pulse repetition frequency (1/s)	Duration of the treatment (s)	Dose (U^2 × On time per burst [V^2 × s])
8 × 100 μs	100	800	800	8	8	327.68
8 × 5 ms	5000	40000	40000	8	8	1600
HF-BP 12–2–2–2	4	864	17280	4320	20	2764.8
HF-BP 22–2–2–2	4	200	10000	2500	50	2500
HF-BP 32–2–2–2	4	128	12800	3200	100	3200

ter of cell membrane was obtained from recorded images. At least 3 images per pulse protocol were analyzed.

2.8. Measurements of pH changes after pulse delivery and temperature monitoring

For measurement of pH changes in 4 mm cuvette after pulse delivery SevenGo-SG2 pH meter and InLab Nano (Mettler-Toledo, Switzerland) measuring electrode were used. 150 μl of cell suspension (1x10^5 cells) were pipetted into 4 mm cuvette and pulses were applied. Immediately after pulse delivery 37.5 μl (25% of volume) of fetal bovine serum (FBS) were added and cell suspensions was mixed by pipetting. Cuvette with cell suspension was placed in water bath heated to 37 °C and pH probe was dipped in cell suspension. pH of cell suspension was measured every minute for 5 min after pulse delivery. Temperature of the cell suspension was monitored during pH measurements using the fiber optic sensor system (opSens, Canada), which consisted of ProSens signal conditioner and a fiber optic temperature sensor OTG-M170 in order to make sure that measured pH changes were not the consequence of temperature changes. Temperature of the sample was also measured during pulse delivery for all five pulse protocols.

2.9. Statistical analysis

All results are reported as a mean value of 3 to 5 experiments. The spread of the data is given by standard deviation. The significance between the experimental groups was analyzed in SigmaPlot 11.0 (Systat Software Inc., Chicago, IL, USA), and determined using One way ANOVA test followed by Tukey's multiple comparison test. The statistically significant difference was assumed at $p < 0.05$.

3. Results

3.1. Permeabilization and cell viability curves

Electroporation experiments resulting in membrane permeabilization and cell viability curves were performed for all five pulse protocols (Fig. 1). Electroporation with applying 8 × 5 ms lead to permeabilization at the lowest electric field; 95% of permeabilized cells were already obtained at 0.75 kV/cm. All three HF-BP pulse protocols and pulse protocol 8 × 100 μs lead to similar permeabilization; 73%–87% of cells were permeabilized at 1 kV/cm. Using pulse protocol 8 × 5 ms also a decrease in cell viability at lower electric fields was observed; less than 10% of cells were viable at 1 kV/cm, while using HF-BP pulse protocols or 8 × 100 μs pulse protocol viability of the cells was better than 80% at the same electric field. Pulse protocol HF-BP 1 and 3 lead to decrease in cell viability at lower electric fields compared to pulse protocol HF-BP 2 and pulse protocol 8 × 100 μs, which ensued similar viability of the cells at electric fields tested; more than 80% of cells were viable at 1.25 kV/cm. The intersection of permeabilization and cell viability curve is where the greatest fraction of cells is permeabilized and cell viability is the highest. The intersection of permeabilization and cell viability curve was at electric fields 0.6, 1.25, 1, 1.20 and 1.05 kV/cm for pulse protocols 8 × 5 ms, 8 × 100 μs, HF-BP 1, HF-BP 2 and HF-BP 3, respectively. Since optimal permeabilization for PI is not necessary also optimal for pDNA uptake we screened the interval of electric fields below and above the intersection of permeabilization and cell viability curves for GET efficiency (data not shown) to choose the final electric field used in every GET pulse protocol. The final electric fields used in GET experiments were 0.5, 1.6, 1, 1.25, 1.25 for pulse protocols 8 × 5 ms, 8 × 100 μs, HF-BP 1, HF-BP 2 and HF-BP 3, respectively.

3.2. Gene electrotransfer

We tested seven different pDNA concentrations: 20, 40, 60, 80, 100, 250 or 500 μg/ml. In all five pulse protocols percent of GFP positive cells increased with increasing pDNA concentration (Fig. 2). Increasing pDNA concentration above 100 μg/ml if pulse protocols 8 × 100 μs or 8 × 5 ms were applied lead to almost no increase in GFP positive cells, contrary to HF-BP pulse protocols where the percent of GFP positive cells with highest pDNA concentrations (250 and 500 μg/ml) increased significantly. When applying HF-BP pulse protocols we were able to obtain around 40% of GFP positive cells.

Percent of GFP positive cells obtained with pulse protocol 8 × 100 μs and pulse protocol 8 × 5 ms was similar at same concentrations of pDNA. With the highest pDNA concentration we successfully transfected around 50% of cells. Also, the transfection efficiency obtained between pulse protocols HF-BP was similar at same concentrations of pDNA. With the lowest concentration of pDNA (20 μg/ml) around 5% of cells were successfully transfected and with the highest concentration (500 μg/ml) around 40%. Exact percent of GET with the highest concentration of pDNA for all five pulse protocols and accompanying viability results are summarized in Table 3.

At the lowest pDNA concentration (20 μg/ml) percent of GFP positive cells was statistically significant higher after GET with pulse protocol 8 × 100 μs and pulse protocol 8 × 5 ms compared to all three pulse protocols HF-BP. When the highest pDNA concentration (500 μg/ml) was used statistically significant difference in percent of GFP positive cells was observed only in GET with pulse protocol 8 × 100 μs and pulse protocol 8 × 5 ms compared to pulse protocol HF-BP 1 and pulse protocol HF-BP 3.

No GFP positive cells were observed in the absence of electric pulses or the absence of pDNA.

3.3. Cell viability after GET

In addition to cell viability measurement in 0–2 kV electric field range in order to get cell viability curves, MTS assay was also performed after every GET experiment at fixed electric field without or

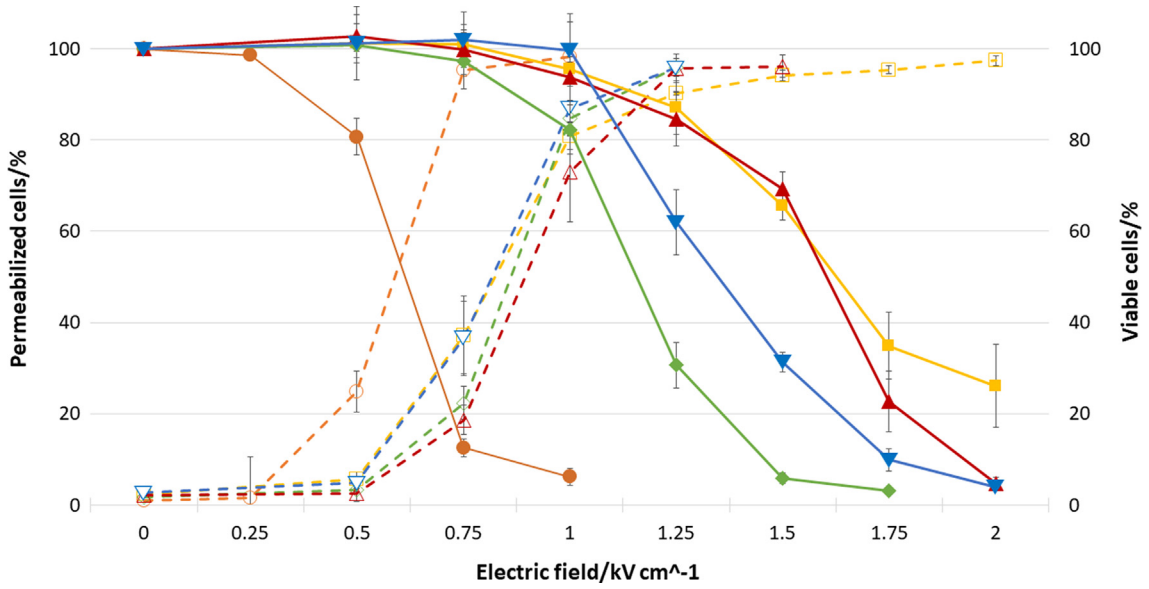

Fig. 1. Permeabilization dashed lines (empty symbols) and cell viability solid lines (filled symbols) for all five pulse protocols used. 8 × 100 μs (yellow □/■); 8 × 5 ms (orange ○/●); HF-BP 1(green ◇/◆); HF-BP 2 (red Δ/▲) and HF-BP 3 (blue ▽/▼). Vertical bars represent standard deviation.

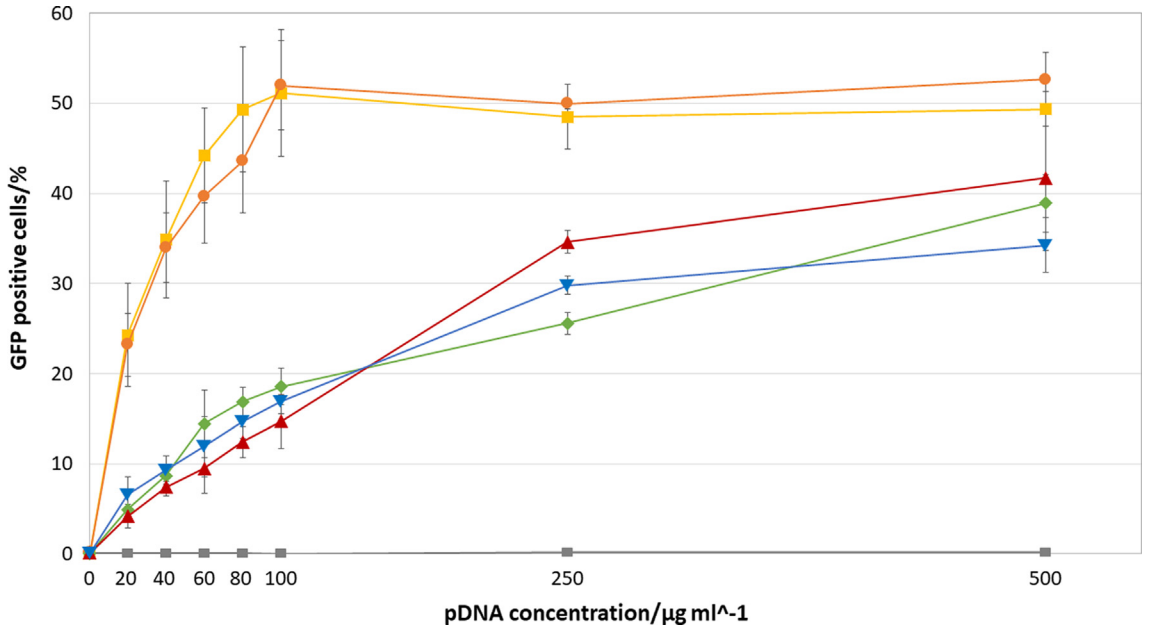

Fig. 2. GET efficiency for all five pulse protocols, 8 × 100 μs (yellow ■); 8 × 5 ms (orange ●); HF-BP 1(green ◆); HF-BP 2 (red ▲) and HF-BP 3 (blue ▼), without and with seven pDNA concentrations, 20, 40, 60, 80, 100, 250 and 500 μg/ml, 0 V – no applied pulses (gray ■). Bars represent standard deviation.

Table 3
Results of GET, viability and overall GET with the highest concentration (500 μg/ml) of pDNA using all five pulse protocols.

Pulse protocol	Electric field (kV/cm)	GET (%)	Viability (%)	Overall GET (%)
8 × 100 μs	1.6	49 ± 1.9	56 ± 5.6	28 ± 3.3
8 × 5 ms	0.5	53 ± 3	75 ± 16.7	40 ± 10.3
HF-BP 1	1	39 ± 3.2	82 ± 6	32 ± 1.6
HF-BP 2	1.25	42 ± 8.1	82 ± 11.8	34 ± 7
HF-BP 3	1.25	34 ± 3.1	72 ± 3.1	25 ± 2.2

with seven pDNA concentrations (Fig. 3). Viability of cells was different among five pulse protocols tested. The lowest cell viability was observed after application of pulse protocol 8 × 100 μs, around 50%. A bit higher viability, around 60%, was obtained when pulse protocol HF-BP 3 was applied. Pulse protocol 8 × 5 ms and pulse protocol HF-BP 1 led to approximately 80% of cell viability. The highest cell viability was observed with pulse protocol HF-BP 2 where nearly 90% of cells were viable 24 h after pulse delivery.

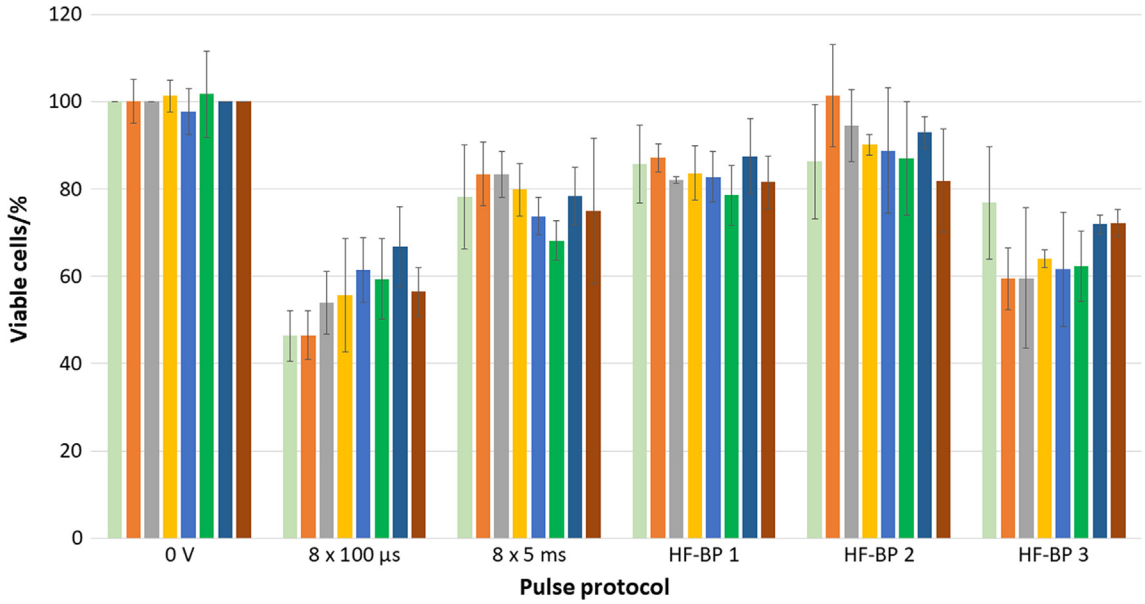

Fig. 3. Cell viability for all five pulse protocols, 8 × 100 µs, 8 × 5 ms, HF-BP 1, HF-BP 2 and HF-BP 3, without (light green) and with seven pDNA concentrations, 20 (orange), 40 (gray), 60 (yellow), 80 (light blue), 100 (dark green), 250 (dark blue) and 500 µg/ml (red), 0 V – no applied pulses. Vertical bars represent standard deviation.

Exact percent of cell viability with the highest concentration of pDNA (500 µg/ml) for all five pulse protocols are summarized in Table 3.

In control cells as well as in cells that were exposed to any of five pulse protocols tested there was no statistically significant difference in cell viability between group with no added pDNA and groups with various pDNA concentrations added in cell suspension. Even in groups in which the highest pDNA concentration (500 µg/ml) was used there was no significant decrease in cell viability observed which shows that pDNA concentration did not have any negative effect on cell viability as detected by MTS cell viability assay.

3.4. Overall gene electrotransfer

Overall GET in percent (Fig. 4) was calculated as % of GFP positive cells multiplied by % of viable cells divided by 100. We can observe that the highest overall gene electrotransfer (GET) (40 ± 10.3%) was achieved with pulse protocol 8 × 5 ms. At the lowest pDNA concentration (20 µg/ml) percent of viable GFP positive cells was statistically significant higher after GET with pulse protocol 8 × 100 µs and pulse protocol 8 × 5 ms compared to all three pulse protocols HF-BP. Percent of GFP positive cells was also significantly higher with pulse protocol 8 × 5 ms compared to pulse protocol 8 × 100 µs.

Overall GET with pulse protocol 8 × 100 µs and all three pulse protocols HF-BP with the highest pDNA concentration was not statistically significant different, it amounted approximately 25–34%. Exact percent of overall GET with the highest concentration of pDNA for all five pulse protocols are summarized in Table 3. When the highest pDNA concentration (500 µg/ml) was used statistically significant difference in percent of viable GFP positive cells was observed only between pulse protocol 8 × 5 ms and pulse protocol HF-BP 3.

3.5. Median fluorescence intensity

Measurements of median fluorescence intensity of GFP positive cells on flow cytometer were also collected for each experiment (Fig. 5). Median fluorescence was the highest when the highest concentration of pDNA was used. In this case maximum median fluorescence of all three pulse protocols HF-BP was similar, while more than double median fluorescence was obtained with pulse protocol 8 × 100 µs and pulse protocol 8 × 5 ms. With pulse protocol 8 × 5 ms higher median fluorescence was measured at pDNA concentrations between 40 µg/ml and 100 µg/ml compared to pulse protocol 8 × 100 µs and pulse protocols HF-BP where more pronounced increase in median fluorescence was observed only with the highest pDNA concentrations, 250 and 500 µg/ml.

Median fluorescence intensity at the lowest (20 µg/ml) and at the highest (500 µg/ml) pDNA concentration was statistically significant higher after GET with pulse protocols 8 × 100 µs and 8 × 5 ms compared to all three pulse protocols HF-BP.

3.6. pDNA interaction with cell membrane

pDNA interaction with cell membrane was visualized following 8 × 100 µs, 8 × 5 ms and HF-BP 2 protocols each with the lowest and the highest pDNA concentrations, 20 µg/ml and 500 µg/ml, respectively. In the absence of pulse delivery no increase in fluorescence intensity alongside cell membrane was observed.

Analyzing fluorescence intensity along cell perimeter following 8 × 100 µs and 8 × 5 ms protocols increased fluorescence intensity was observed only on one side of cell membrane representing formation of pDNA aggregates on cell membrane facing the cathode (Figs. 6, B and 7, B). After 8 × 100 µs pulse protocol pDNA aggregates on cell membrane were visible after GET with both pDNA concentrations, 20 µg/ml (Fig. 6, A) and 500 µg/ml (Fig. 6, D). Peak in average fluorescence intensity after 8 × 100 µs protocol with 500 µg/ml of pDNA was significantly (10 times) higher than average peak in fluorescence intensity after 8 × 100 µs protocol with 20 µg/ml of pDNA (Fig. 6, C).

pDNA aggregates on cell membrane after 8 × 5 ms pulse protocol with both pDNA concentrations, 20 µg/ml and 500 µg/ml, are shown in Fig. 7, A and D respectively. Peak in fluorescence intensity after 8 × 5 ms protocol with 20 µg/ml of pDNA was almost the same as peak in fluorescence intensity after 8 × 100 µs protocol with 500 µg/ml of pDNA. Peak in fluorescence intensity after 8 × 5 ms protocol with 500 µg/ml of pDNA was significantly

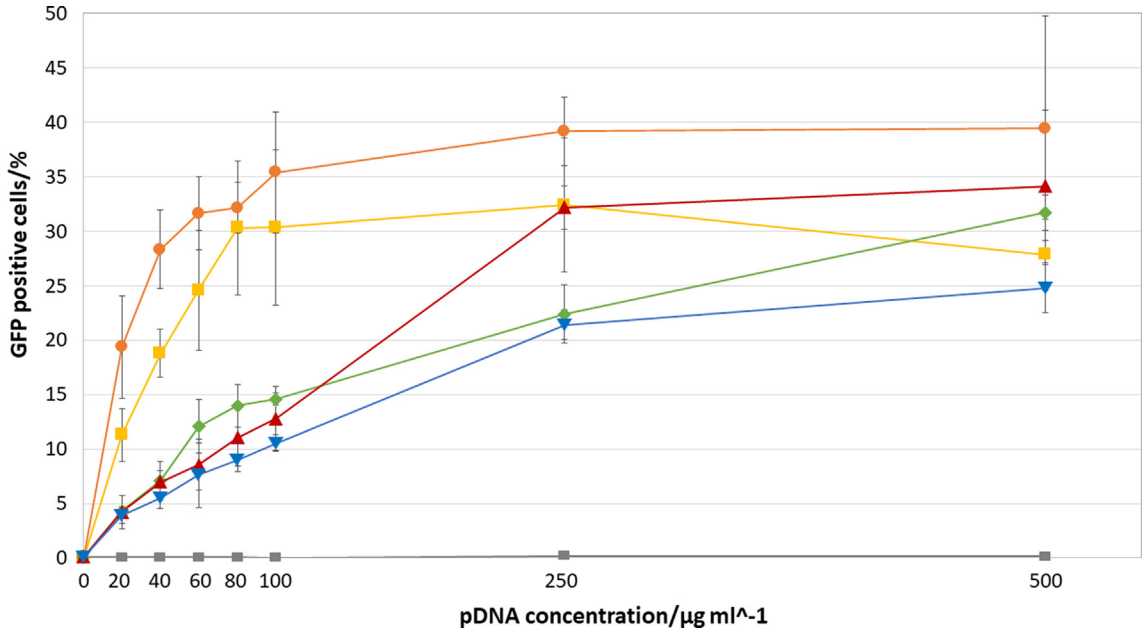

Fig. 4. Overall GET efficiency for all five pulse protocols 8 × 100 µs (yellow ■); 8 × 5 ms (orange ●); HF-BP 1(green ◆); HF-BP 2 (red ▲) and HF-BP 3 (blue ▼), without and with seven pDNA concentrations, 20, 40, 60, 80, 100, 250 and 500 µg/ml, 0 V – no applied pulses (gray ■). Vertical bars represent standard deviation.

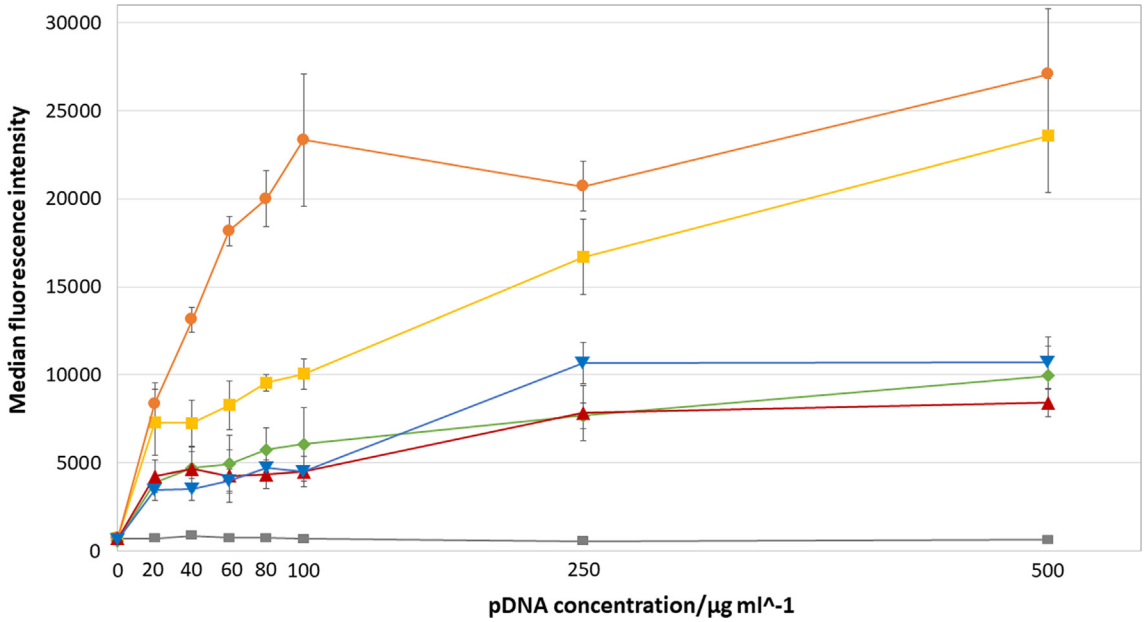

Fig. 5. Median fluorescence intensity for all 5 pulse protocols, 8 × 100 µs (yellow ■); 8 × 5 ms (orange ●); HF-BP 1(green ◆); HF-BP 2 (red ▲) and HF-BP 3 (blue ▼), without and with seven pDNA concentrations, 20, 40, 60, 80, 100, 250 and 500 µg/ml, 0 V – no applied pulses (gray ■). Vertical bars represent standard deviation.

(almost 3 times) higher compared to the peak in fluorescence intensity with 20 µg/ml of pDNA (Fig. 7, C).

Analyzing fluorescence intensity alongside cell perimeter after HF-BP 2 protocol two peaks in fluorescence intensity were observed representing formation of pDNA aggregates on both sides of cell membrane facing the electrodes. The peaks were distinct when 500 µg/ml of pDNA was used and hard to notice after HF-BP 2 protocol with 20 µg/ml of pDNA (Fig. 8, B). Statistical analysis of peaks in fluorescence intensity showed significantly higher fluorescence in both peaks compared to background fluorescence at both pDNA concentrations. The two peaks in fluorescence intensity were not significantly different, however, slightly lower fluorescence was observed at peak 1 with both pDNA concentrations used (Fig. 8, C). Up to 7 times higher peak in fluorescence intensity was observed when 500 µg/ml of pDNA was added compared to when 20 µg/ml of pDNA was added. Peak fluorecence intensity after 8 × 100 µs pulse protocol with with 500 µg/ml of pDNA was also significantly higher compared to peak in fluorescence intensity after HF-BP 2 protocol with 20 µg/ml and 500 µg/ml of pDNA. Application of 8 × 100 µs protocol with 20 µg/ml of pDNA resulted in an average peak in fluorescence intensity only a little higher compared to peak in fluorescence intensity after HF-BP 2 protocol with 20 µg/ml of pDNA and lower compared to peak in fluorescence intensity after HF-BP 2 protocol with 500 µg/ml of pDNA.

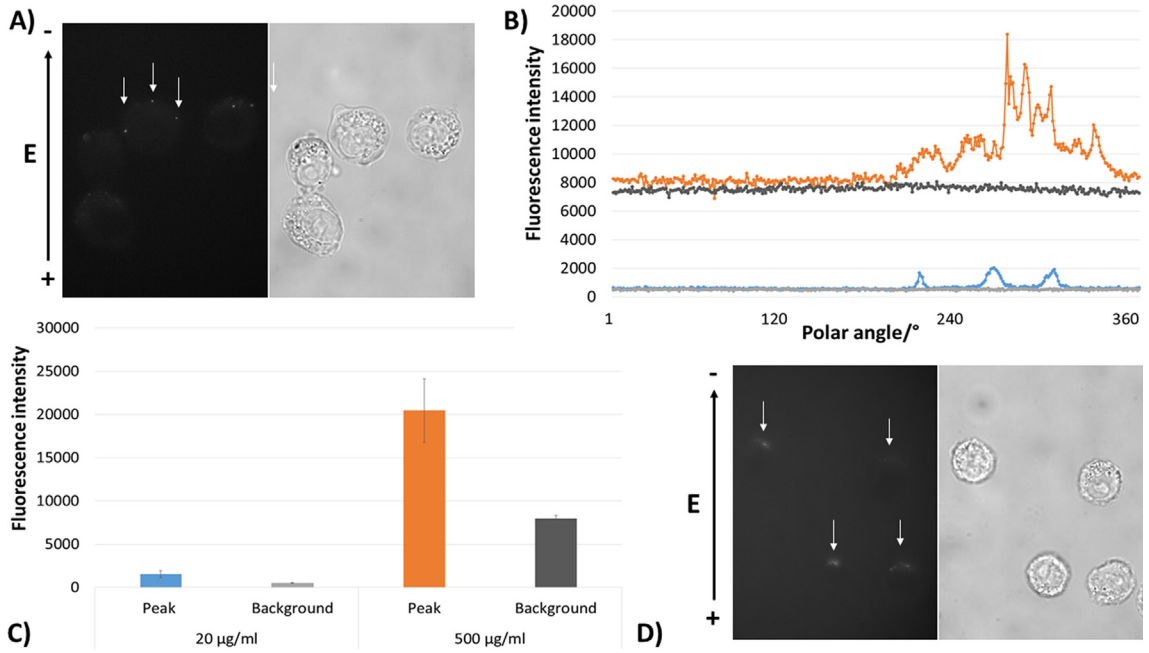

Fig. 6. pDNA interaction with cell membrane after 8 × 100 µs pulse protocol. A) Images of brightfield and TOTO-1 fluorescence taken under the microscope, with 20 µg/ml or D) 500 µg/ml of pDNA. B) TOTO-1 fluorescence measured along perimeter of cell membrane of a single cell. 20 µg/ml of pDNA (blue); background 20 µg/ml (light gray); 500 µg/ml of pDNA (orange); background 500 µg/ml (dark gray). C) Average TOTO-1 fluorescence intensity at peaks measured on 5 cells. Vertical bars represent standard deviation.

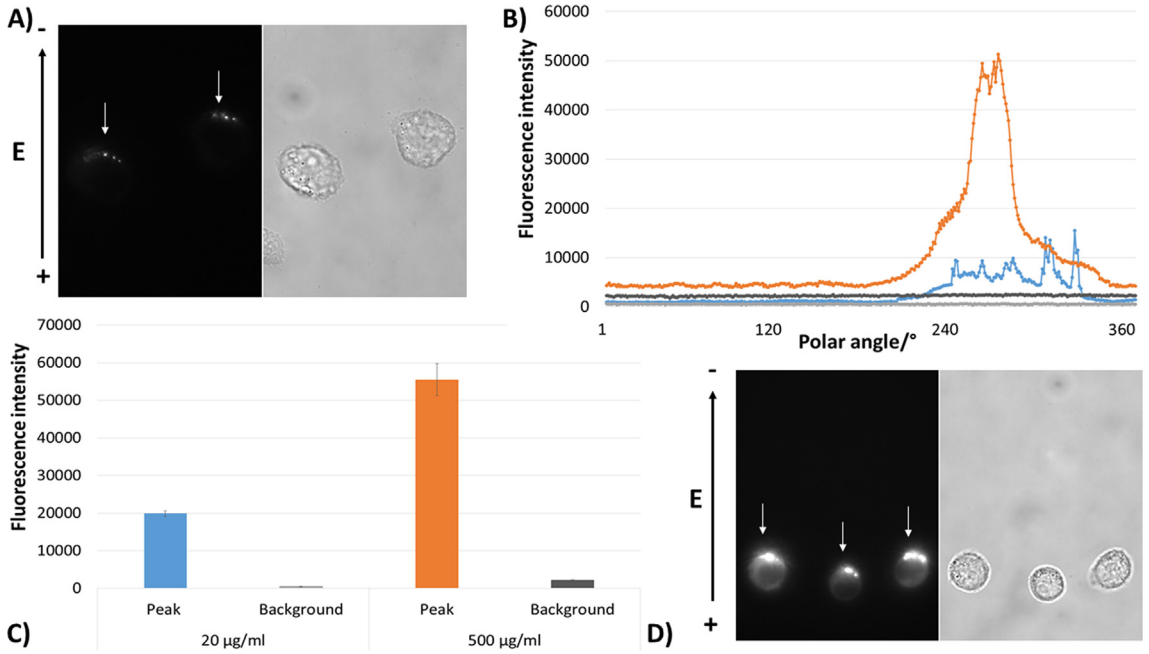

Fig. 7. pDNA interaction with cell membrane after 8 × 5 ms pulse protocol. A) Images of brightfield and TOTO-1 fluorescence taken under the microscope, with 20 µg/ml or D) 500 µg/ml of pDNA. B) TOTO-1 fluorescence measured along perimeter of cell membrane of a single cell. 20 µg/ml of pDNA (blue); background 20 µg/ml (light gray); 500 µg/ml of pDNA (orange); background 500 µg/ml (dark gray). C) Average TOTO-1 fluorescence intensity at peaks measured on 5 cells. Vertical bars represent standard deviation.

Following application of 8 × 5 ms protocol with 20 µg/ml of pDNA average peak in fluorescence intensity was significantly higher compared to the peaks in fluorescence intensity after HF-BP 2 protocol with both pDNA concentrations and 8 × 100 µs protocol with 20 µg/ml of pDNA.

3.7. pH and temperature measurements

We measured pH changes after pulse delivery in the middle of 4 mm cuvettes according to gene electrotransfer protocol; i.e. at fixed temperature of 37 °C for 5 min (Fig. 9). After pulse delivery

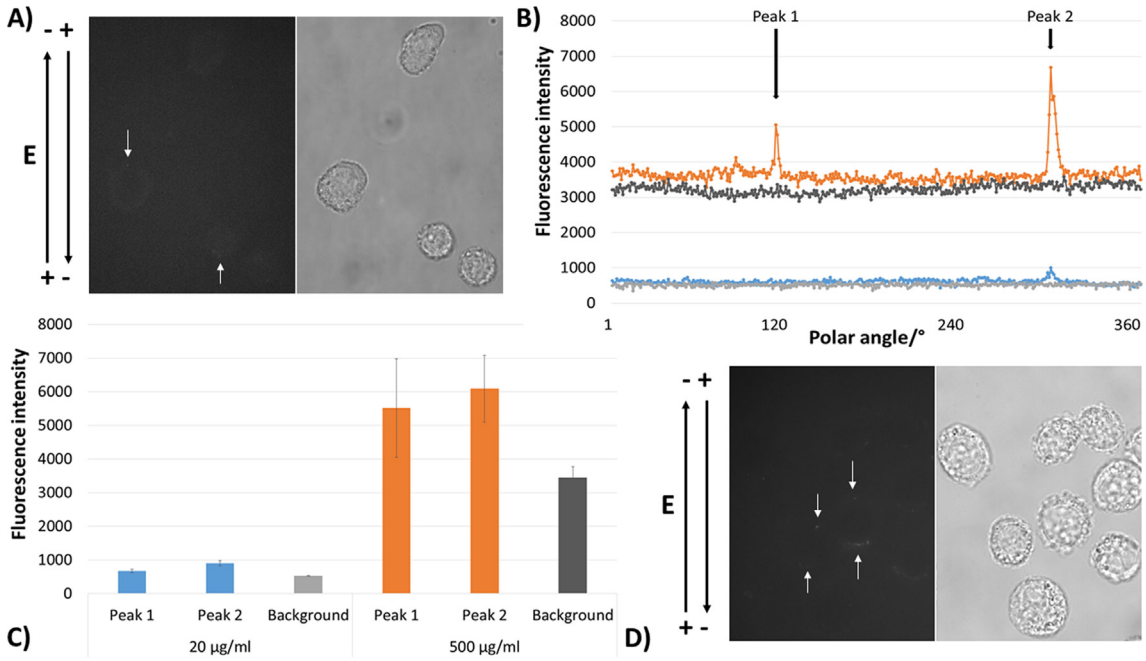

Fig. 8. pDNA interaction with cell membrane after HF-BP 2 pulse protocol. A) Images of brightfield and TOTO-1 fluorescence taken under the microscope, with 20 µg/ml or D) 500 µg/ml of pDNA. B) TOTO-1 fluorescence measured along perimeter of cell membrane of a single cell. 20 µg/ml of pDNA (blue); background 20 µg/ml (light gray); 500 µg/ml of pDNA (orange); background 500 µg/ml (dark gray). C) Average TOTO-1 fluorescence intensity at peaks measured on 5 cells. Vertical bars represent standard deviation.

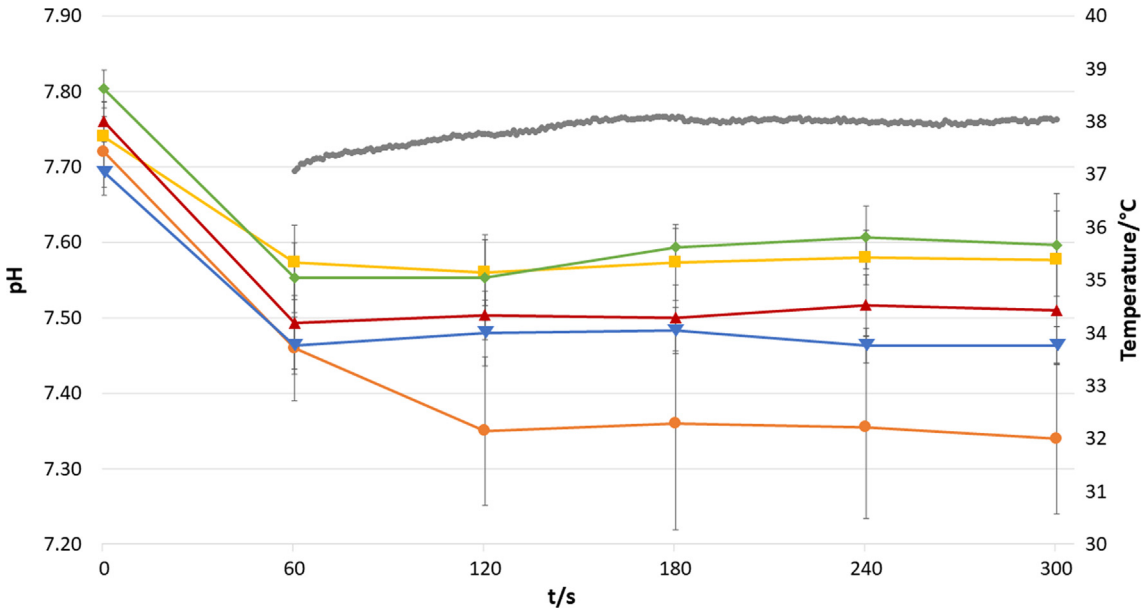

Fig. 9. Cell suspension pH changes for all five pulse protocols used, 8 × 100 µs (yellow ■); 8 × 5 ms (orange ●); HF-BP 1 (green ◆); HF-BP 2 (red ▲) and HF-BP 3 (blue ▼). Vertical bars represent standard deviation. Also shown is example of temperature (gray ●) monitoring during pH measurement.

we also added FBS and mixed cells by pipetting, following protocol for GET, therefore local pH changes in the cuvette were blurred.

Electroporation statistically significant decreased pH in average in overall suspension of cells. Decrease in pH of 0.17–0.27 was measured first minute after pulse delivery in all five pulse protocols tested. pH remained constantly lower all 5 min after pulse delivery in all pulse protocols tested except 8 × 5 ms pulse protocol. Using 8 × 5 ms pulse protocol pH additionally decreased for 0.11 in the second minute after pulse delivery and remained constant then after. When comparing pH changes following different pulse protocols in 5 min after pulse delivery statistically significant difference was observed at 2, 3, 4 and 5 min after electroporation between pulse protocol 8 × 5 ms and pulse protocols 8 × 100 µs and HF-BP 1. At every time point pH after delivery of pulse protocol 8 × 5 ms was significantly lower compared to pH after delivery of pulse protocol 8 × 100 µs or pulse protocol HF-BP 1. However, although the decrease was statistically significant the observed drop in pH was not large. The lowest measured pH values were still above 7.2.

For each tested pulse parameter sample temperature increase during pulse delivery was measured. All experiments were done at room temperature that was approximately 25.5 °C. The highest

temperature of 30.6 °C was recorded after application of HF-BP 1 pulse parameters. Measured temperature increases after delivery of 8 × 100 μs, 8 × 5 ms, HF-BP 1, HF-BP 2 and HF-BP 3 pulse parameters were 0.8 °C, 2.4 °C, 5.1 °C, 3.1 °C and 3.6 °C, respectively (Supplementary Fig. 2).

4. Discussion

The results of our study confirm that with HF-BP pulses we can achieve successful GET with bipolar microsecond pulses *in vitro* with sufficiently high pDNA concentration. The electric field chosen for GET with pulse protocols HF-BP was in the range of electric fields used for GET with longer monopolar pulses. GET efficiency increased with increasing pDNA concentration. However, in attempt to achieve GET efficiency comparable to that of longer monopolar pulses (8 × 100 μs and 8 × 5 ms pulse protocols) 5 times higher pDNA concentration was needed for GET with HF-BP pulse protocols. Further optimization of HF-BP pulse protocols could lessen the need for high pDNA concentrations. Nevertheless, presented results potentially open completely new field of possible GET applications – less painful and widely accepted GET applications, like nucleic acid-based vaccination.

Electric field required for successful GET using protocols HF-BP (1.25 kV/cm) was lower than electric field required for GET with pulse protocol 8 × 100 μs (1.6 kV/cm) and 2.5 times higher than electric field required for GET with pulse protocol 8 × 5 ms (0.5 kV/cm). This is in contrast with previously published data [53,54,59] showing that higher electric fields are required when applying HF-BP pulses. However, previous studies were performed with HF-BP pulse protocols that had the same on-time per treatment as 8 × 100 μs. In our experiments we extended on-time per treatment in HF-BP pulse protocols (12–21x) compared to 8 × 100 μs and thus were able to achieve permeabilization and GET at lower electric filed. In HF-BP pulse protocols on-time per treatment was still more than 2x shorter as in 8 × 5 ms pulse protocol. On-time per treatment was prolonged with increased number of pulses in each burst of HF-BP pulse protocols. This might be the explanation for lower electric field required for GET with HF-BP pulse protocols as it was previously shown that with increased number of pulses, the electric field needed to obtain the same fraction of electroporated cells decreases [82].

In order to investigate if the lack of electrophoretic force during HF-BP pulse delivery can be compensated with higher pDNA concentration we tested the effect of increasing pDNA concentration on cell viability and GET efficiency. The addition of pDNA in cell suspension was not toxic regardless of the concentration used (Fig. 3). Moreover, even the highest pDNA concentration (500 μg/ml) did not decrease cell viability, alone or in combination with applying any of five pulse protocols tested as detected by MTS assay 24 h after GET. Our results are comparable to results obtained in [83] where it was shown that pDNA concentrations up to 1 mg/ml did not decrease survival of mesenchymal stem cells. However, some studies report that pDNA concentrations above 100 μg/ml already have reduced cell survival [84,85] as a consequence of cell defense mechanisms activation triggered by pDNA entrance leading to programmed cell death [86,87].

Our results show that percent of GFP positive cells was increasing with increasing pDNA concentration. Increase was more pronounced when HF-BP pulse protocols were applied. With the highest two pDNA concentrations (250 and 500 μg/ml) the increase in percent of GFP positive cells was significant in all three HF-BP pulse protocols. Contrary to pulse protocol 8 × 100 μs and pulse protocol 8 × 5 ms where no further increase in percent of GFP positive cells with pDNA concentrations above 60 μg/ml or 80 μg/ml was observed (Fig. 2). Similar trend was observed for overall GET with the highest pDNA concentration (500 μg/ml). Overall GET obtained by HF-BP pulse protocols was comparable to overall GET obtained by "classical", long monopolar pulse protocols (Fig. 4). It was already shown that with higher pDNA concentration successful GET is possible also with shorter high voltage pulses where weaker electrophoretic forces are present [34,39,88]. This is in agreement with our results obtained with HF-BP pulse protocols where with higher pDNA concentration we were able to achieve comparable GET efficiency in the absence of net electrophoretic force on pDNA. According to findings of [40] the diffusion coefficient of circular 4.7 kbp large pDNA used in our study is similar at all tested concentrations (20 to 500 μg/ml).

Protein expression following transfection is regulated by a number of factors, including the promoter used, pDNA copy number within the cell and the availability of cellular machinery for transcription and translation. Fluorescence intensity of the cell is considered to be indicative of the number of pDNA copies inside the cell that have reached the cell nucleus and have been successfully transcribed and translated into fluorescent proteins [89,90]. Our results of median fluorescence intensity thus suggest that the lack of electrophoretic force can only partially be compensated with higher pDNA concentration. Median fluorescence intensity with the lowest (20 μg/ml) and the highest (500 μg/ml) pDNA concentration was significantly higher after GET with pulse protocols 8 × 100 μs and 8 × 5 ms compared to all three pulse protocols HF-BP (Fig. 5). Suggesting that although with the highest pDNA concentration (500 μg/ml) we were able to achieve similar percent of transfected cells, the number of pDNA copies that were successfully transfected into cells was higher when pulse protocols 8 × 100 μs and 8 × 5 ms were used. This indicates that electrophoretic force is also instrumental in pDNA translocation across cell membrane.

Recently in a study reported by [88] authors observed increase in GET with increasing pDNA concentration and that at some point GET efficiency no longer increases with higher pDNA concentration. They also reported that if pulse parameters are suboptimal this plateau in GET efficiency is not observed. However, contrary to our results, they observed decrease in cell survival with increasing pDNA concentration. Reason for this might be that different assays for cell survival were used. We used MTS assay which measures cell viability 24 h after experiments, and they did clonogenic assay which is a cell survival assay based on the ability of a single cell to grow into a colony.

Direct observation of pDNA aggregates formation on cell membrane showed that increasing pDNA concentration also increases the fluorescence intensity of pDNA aggregates labeled with TOTO-1 nucleic acid stain formed on cell membrane. Florescence intensity of pDNA aggregates depends also on duration of applied pulses. With the lowest pDNA concentration (20 μg/ml) the fluorescence intensity of pDNA aggregates formed on cell membrane following 8 × 5 ms pulse protocol (Fig. 7) was almost 4 times higher as fluorescence intensity of pDNA aggregates formed after HF-BP 2 pulse protocol (Fig. 8) with the highest pDNA concentration (500 μg/ml) and comparable to 8 × 100 μs pulse protocol (Fig. 6) with the highest pDNA concentration. However, we did not observe any direct correlation between fluorescence intensity of pDNA aggregates formed on cell membrane and transfection efficiency. With the highest pDNA concentration used, fluorescence intensity of pDNA aggregates formed after HF-BP 2 pulse protocol was almost 10 times lower compared to fluorescence intensity of pDNA aggregates formed after 8 × 5 ms protocol while no significant difference was observed in percent of GFP positive cells. Similar observations were reported previously [91]. The interaction of pDNA with cell membrane is only one of several steps and barriers that pDNA has to overcome in order to be expressed. Other factors

such as pDNA stability in cytoplasm, its transport to perinuclear region and successful crossing of nuclear envelope are also crucial and contribute to differences in transfection efficiency [18].

Since application of bipolar pulses also comes with decreased electrochemical reactions [92,93], and lower metal release from electrodes [59], we measured pH changes of overall cell suspension after pulse delivery. To mimic our experimental protocol with cells FBS was added after pulse delivery to increase cell survival [78] and cell suspension was mixed by pipetting. Cell suspension in cuvette was placed in water bath heated to 37 °C. We observed slight decrease in pH of cell suspension, but not large enough to affect cell membrane resealing dynamics [94]. This drop in pH was stable during 5 min following pulse delivery in all pulse protocols tested except pulse protocol 8 × 5 ms where pH additionally decreased in the second minute after pulse delivery and remained constant then after. Significant drop in pH was observed after pulse protocol 8 × 5 ms compared to pH after delivery of pulse protocol 8 × 100 μs and pulse protocol HF-BP 1 (Fig. 9). Our measurements are in agreement with [92], where it was shown that longer pulses lead to more electrochemical reactions which cause changes in the chemical composition of electroporation medium or pH. According to our results larger pH changes must be occurring at anode side since the overall pH decreased after pulse delivery. This is in agreement with [45] where larger extension of the anodic pH front relative to the cathodic one was observed. Another explanation for slight decrease in medium pH can be the repair mechanisms of cells which are activated in order to repair damage caused on cell membrane during electric field delivery. This mechanisms include exocytosis of lysosomes and the release of their acidic content in cell surroundings [95]. Cell lysis could also contribute to observed decrease in pH since intracellular pH is around 7.0–7.2 [96].

Temperature is reported to affect cell membrane fluidity, consequently permeabilization [97] and GET efficiency [98,99]. However, final temperature of the electroporated cell samples measured during delivery of different pulse protocols in our study was not higher than 37 °C which was the temperature of after pulse incubation. Therefore, we conclude that temperature increase during pulse delivery had no observable effect on GET efficiency.

We did not observe any difference in efficiency between all three HF-BP protocols tested. Changing number of bursts or number of pulses in each burst in the tested range of parameters did not lead to increased GET efficiency. Minor differences were observed in cell viability 24 h after pulse delivery where both increased number of bursts and increased number of pulses in burst lead to slightly lower cell viability, although not statistically significant.

5. Conclusions

Successful GET can be achieved with HF-BP bipolar microsecond pulses. The efficiency increases with increasing pDNA concentration however, number of transferred plasmid copies seems to be higher with longer monopolar pulses. Prolonged on-time per treatment with increased number of pulses in each burst or increased number of bursts enabled comparable overall GET with HF-BP pulse protocols at lower electric field compared to pulse protocol 8 × 100 μs. According to reports using similar HF-BP pulse protocols where even at double stimulating voltage eightfold reduction in muscle contraction intensity was observed [51,77], we can conclude that widely accepted GET applications, like nucleic acid-based vaccination, are feasible. However, achieving sufficiently high pDNA concentrations in tissue can be challenging.

Declaration of Competing Interest

The authors declare that they have no known competing financial interests or personal relationships that could have appeared to influence the work reported in this paper.

Acknowledgments

This research was supported by Slovenian Research Agency (ARRS) [research core funding No. P2-0249, and funding for Junior Researcher to TP]. Experiments were performed within Infrastructure Program: Network of research infrastructure centers at University of Ljubljana (MRIC UL IP-0510). Authors would like to thank L. Vukanović and D. Hodžić for their help in the cell culture laboratory. Authors would also like to thank A. Cvetkoska and dr. E. Pirc for their help with pulse recording and image production.

Appendix A. Supplementary data

Supplementary data to this article can be found online at https://doi.org/10.1016/j.bioelechem.2021.107803.

References

[1] L. Rems, M. Tarek, M. Casciola, D. Miklavčič, Properties of lipid electropores II: Comparison of continuum-level modeling of pore conductance to molecular dynamics simulations, Bioelectrochemistry 112 (2016) 112–124, https://doi.org/10.1016/j.bioelechem.2016.03.005.
[2] T. Kotnik, L. Rems, M. Tarek, D. Miklavcic, Membrane Electroporation and Electropermeabilization: Mechanisms and Models, Annu. Rev. Biophys. 48 (2019) 63–91, https://doi.org/10.1146/annurev-biophys-052118-115451.
[3] J.C. Weaver, Y.A. Chizmadzhev, Theory of electroporation: A review, Bioelectrochem. Bioenerg. 41 (1996) 135–160, https://doi.org/10.1016/S0302-4598(96)05062-3.
[4] M.L. Yarmush, A. Golberg, G. Serša, T. Kotnik, D. Miklavčič, Electroporation-based technologies for medicine: Principles, applications, and challenges, Annu. Rev. Biomed. Eng. 16 (2014) 295–320, https://doi.org/10.1146/annurev-bioeng-071813-104622.
[5] B. Geboers, H.J. Scheffer, P.M. Graybill, A.H. Ruarus, S. Nieuwenhuizen, R.S. Puijk, P.M. Van Den Tol, R.V. Davalos, B. Rubinsky, T.D. De Gruijl, D. Miklavčič, M.R. Meijerink, High-voltage electrical pulses in oncology: Irreversible electroporation, electrochemotherapy, gene electrotransfer, electrofusion, and electroimmunotherapy, Radiol. Soc. North Am. (RSNA) (2020), https://doi.org/10.1148/radiol.2020192190.
[6] T. Kotnik, W. Frey, M. Sack, S. Haberl Meglič, M. Peterka, D. Miklavčič, Electroporation-based applications in biotechnology, Trends Biotechnol. 33 (2015) 480–488, https://doi.org/10.1016/j.tibtech.2015.06.002.
[7] S. Mahnič-Kalamiza, E. Vorobiev, D. Miklavčič, Electroporation in Food Processing and Biorefinery, J. Membr. Biol. 247 (2014) 1279–1304, https://doi.org/10.1007/s00232-014-9737-x.
[8] A. Golberg, M. Sack, J. Teissie, G. Pataro, U. Pliquett, G. Saulis, T. Stefan, D. Miklavcic, E. Vorobiev, W. Frey, Energy-efficient biomass processing with pulsed electric fields for bioeconomy and sustainable development, Biotechnol. Biofuels 9 (2016), https://doi.org/10.1186/s13068-016-0508-z.
[9] B. Mali, T. Jarm, M. Snoj, G. Sersa, D. Miklavcic, Antitumor effectiveness of electrochemotherapy: A systematic review and meta-analysis, Eur. J. Surg. Oncol. 39 (2013) 4–16, https://doi.org/10.1016/j.ejso.2012.08.016.
[10] L.G. Campana, I. Edhemovic, D. Soden, A.M. Perrone, M. Scarpa, L. Campanacci, M. Cemazar, S. Valpione, D. Miklavčič, S. Mocellin, E. Sieni, G. Sersa, Electrochemotherapy – Emerging applications technical advances, new indications, combined approaches, and multi-institutional collaboration, Eur. J. Surg. Oncol. 45 (2019) 92–102, https://doi.org/10.1016/j.ejso.2018.11.023.
[11] R.V. Davalos, L.M. Mir, B. Rubinsky, Tissue ablation with irreversible electroporation, Ann. Biomed. Eng. 33 (2005) 223–231, https://doi.org/10.1007/s10439-005-8981-8.
[12] A. Sugrue, V. Vaidya, C. Witt, C.V. DeSimone, O. Yasin, E. Maor, A.M. Killu, S. Kapa, C.J. McLeod, D. Miklavčič, S.J. Asirvatham, Irreversible electroporation for catheter-based cardiac ablation: a systematic review of the preclinical experience, J. Interv. Card. Electrophysiol. 55 (2019) 251–265, https://doi.org/10.1007/s10840-019-00574-3.
[13] E. Maor, A. Sugrue, C. Witt, V.R. Vaidya, C.V. DeSimone, S.J. Asirvatham, S. Kapa, Pulsed electric fields for cardiac ablation and beyond: A state-of-the-art review, Hear. Rhythm. 16 (2019) 1112–1120, https://doi.org/10.1016/j.hrthm.2019.01.012.
[14] H.J. Scheffer, K. Nielsen, M.C. De Jong, A.A.J.M. Van Tilborg, J.M. Vieveen, A. Bouwman, S. Meijer, C. Van Kuijk, P. Van Den Tol, M.R. Meijerink, Irreversible electroporation for nonthermal tumor ablation in the clinical setting: A

systematic review of safety and efficacy, J. Vasc. Interv. Radiol. 25 (2014) 997–1011, https://doi.org/10.1016/j.jvir.2014.01.028.
[15] V.Y. Reddy, A. Anic, J. Koruth, J. Petru, M. Funasako, K. Minami, T. Breskovic, I. Sikiric, S.R. Dukkipati, I. Kawamura, P. Neuzil, Pulsed Field Ablation in Patients With Persistent Atrial Fibrillation, J. Am. Coll. Cardiol. 76 (2020) 1068–1080, https://doi.org/10.1016/j.jacc.2020.07.007.
[16] A.R. Denet, R. Vanbever, V. Préat, Skin electroporation for transdermal and topical delivery, Adv. Drug Deliv. Rev. 56 (2004) 659–674, https://doi.org/10.1016/j.addr.2003.10.027.
[17] B. Zorec, V. Préat, D. Miklavčič, N. Pavšelj, Active enhancement methods for intra- and transdermal drug delivery: A review, Zdr. Vestn. 82 (2013) 339–356.
[18] C. Rosazza, S. Haberl Meglic, A. Zumbusch, M.-P. Rols, D. Miklavcic, Gene Electrotransfer: A Mechanistic Perspective, Curr. Gene Ther. 16 (2016) 98–129, https://doi.org/10.2174/1566523216666160331130040.
[19] L. Pasquet, S. Chabot, E. Bellard, B. Markelc, M.P. Rols, J.P. Reynes, G. Tiraby, F. Couillaud, J. Teissie, M. Golzio, Safe and efficient novel approach for non-invasive gene electrotransfer to skin, Sci. Rep. 8 (2018), https://doi.org/10.1038/s41598-018-34968-6.
[20] L. Lambricht, A. Lopes, S. Kos, G. Sersa, V. Préat, G. Vandermeulen, Clinical potential of electroporation for gene therapy and DNA vaccine delivery, Expert Opin. Drug Deliv. 13 (2016) 295–310, https://doi.org/10.1517/17425247.2016.1121990.
[21] L.C. Heller, R. Heller, Electroporation Gene Therapy Preclinical and Clinical Trials for Melanoma, Curr. Gene Ther. 10 (2010) 312–317, https://doi.org/10.2174/156652310791823489.
[22] N.Y. Sardesai, D.B. Weiner, Electroporation delivery of DNA vaccines: Prospects for success, Curr. Opin. Immunol. 23 (2011) 421–429, https://doi.org/10.1016/j.coi.2011.03.008.
[23] J.L. Young, D.A. Dean, Electroporation-Mediated Gene Delivery, Adv. Genet. 89 (2015) 49–88, https://doi.org/10.1016/bs.adgen.2014.10.003.
[24] J. Glasspool-Malone, S. Somiari, J.J. Drabick, R.W. Malone, Efficient nonviral cutaneous transfection, Mol. Ther. 2 (2000) 140–146, https://doi.org/10.1006/mthe.2000.0107.
[25] B. Ferraro, Y.L. Cruz, D. Coppola, R. Heller, Intradermal delivery of plasmid VEGF165 by electroporation promotes wound healing, Mol. Ther. 17 (2009) 651–657, https://doi.org/10.1038/mt.2009.12.
[26] L.M. Mir, M.F. Bureau, J. Gehl, R. Rangara, D. Rouy, J.M. Caillaud, P. Delaere, D. Branellec, B. Schwartz, D. Scherman, High-efficiency gene transfer into skeletal muscle mediated by electric pulses, Proc. Natl. Acad. Sci. U. S. A. 96 (1999) 4262–4267, https://doi.org/10.1073/pnas.96.8.4262.
[27] J. Teissie, M. Golzio, M.P. Rols, Mechanisms of cell membrane electropermeabilization: A minireview of our present (lack of ?) knowledge, Biochim. Biophys. Acta - Gen. Subj. 1724 (2005) 270–280, https://doi.org/10.1016/j.bbagen.2005.05.006.
[28] R.S. Son, K.C. Smith, T.R. Gowrishankar, P.T. Vernier, J.C. Weaver, Basic Features of a Cell Electroporation Model: Illustrative Behavior for Two Very Different Pulses, J. Membr. Biol. 247 (2014) 1209–1228, https://doi.org/10.1007/s00232-014-9699-z.
[29] C. Faurie, M. Rebersek, M. Golzio, M. Kanduser, J.M. Escoffre, M. Pavlin, J. Teissie, D. Miklavcic, M.P. Rols, Electro-mediated gene transfer and expression are controlled by the life-time of DNA/membrane complex formation, J. Gene Med. 12 (2010) 117–125, https://doi.org/10.1002/jgm.1414.
[30] S. Sachdev, S. Feijoo Moreira, Y. Keehnen, L. Rems, M.T.M.T. Kreutzer, P.E.P.E. Boukany, DNA-membrane complex formation during electroporation is DNA size-dependent, Biochim. Biophys. Acta - Biomembr. 1862 (2020), https://doi.org/10.1016/j.bbamem.2019.183089.
[31] M. Wu, F. Yuan, Membrane binding of plasmid DNA and endocytic pathways are involved in electrotransfection of mammalian cells, PLoS ONE 6 (2011), https://doi.org/10.1371/journal.pone.0020923.
[32] C.C. Chang, M. Wu, F. Yuan, Role of specific endocytic pathways in electrotransfection of cells, Mol. Ther. - Methods Clin. Dev. 1 (2014) 14058, https://doi.org/10.1038/mtm.2014.58.
[33] C. Rosazza, H. Deschout, A. Buntz, K. Braeckmans, M.P. Rols, A. Zumbusch, Endocytosis and Endosomal Trafficking of DNA After Gene Electrotransfer In Vitro, Mol. Ther. - Nucleic Acids. 5 (2016), https://doi.org/10.1038/mtna.2015.59 e286.
[34] M. Pavlin, K. Flisar, M. Kandušer, The role of electrophoresis in gene electrotransfer, J. Membr. Biol. 236 (2010) 75–79, https://doi.org/10.1007/s00232-010-9276-z.
[35] F.M. André, J. Gehl, G. Sersa, V. Préat, P. Hojman, J. Eriksen, M. Golzio, M. Cemazar, N. Pavselj, M.P. Rols, D. Miklavcic, E. Neumann, J. Teissié, L.M. Mir, Efficiency of high- and low-voltage pulse combinations for gene electrotransfer in muscle, liver, tumor, and skin, Hum. Gene Ther. 19 (2008) 1261–1271, https://doi.org/10.1089/hum.2008.060.
[36] S. Satkauskas, F. Andre, M.F. Bureau, D. Scherman, D. Miklavcic, L.M. Mir, Electrophoretic Component of Electric Pulses Determines the Efficacy of In Vivo DNA Electrotransfer, Hum. Gene Ther. 16 (2005), https://doi.org/10.1089/hum.2005.16.1194, 050926062340001.
[37] E. Tekle, R.D. Astumian, P.B. Chock, Electroporation by using bipolar oscillating electric field: An improved method for DNA transfection of NIH 3T3 cells, Proc. Natl. Acad. Sci. U. S. A. 88 (1991) 4230–4234, https://doi.org/10.1073/pnas.88.10.4230.
[38] M. Reberšek, C. Faurie, M. Kandušer, S. Korović, J. Teissié, M.P. Rols, D. Miklavčič, Electroporator with automatic change of electric field direction improves gene electrotransfer in-vitro, Biomed. Eng. Online 6 (2007), https://doi.org/10.1186/1475-925X-6-25.
[39] M. Kandušer, D. Miklavčič, M. Pavlin, Mechanisms involved in gene electrotransfer using high- and low-voltage pulses - An in vitro study, Bioelectrochemistry 74 (2009) 265–271, https://doi.org/10.1016/j.bioelechem.2008.09.002.
[40] R.M. Robertson, D.E. Smith, Self-diffusion of entangled linear and circular DNA molecules: Dependence on length and concentration, Macromolecules 40 (2007) 3373–3377, https://doi.org/10.1021/ma070051h.
[41] S. Mahnič-Kalamiza, D. Miklavčič, Scratching the electrode surface: Insights into a high-voltage pulsed-field application from in vitro & in silico studies in indifferent fluid, Electrochim. Acta 363 (2020), https://doi.org/10.1016/j.electacta.2020.137187.
[42] M. Faroja, M. Ahmed, L. Appelbaum, E. Ben-David, M. Moussa, J. Sosna, I. Nissenbaum, S. Nahum Goldberg, Irreversible electroporation ablation: Is all the damage nonthermal?, Radiology 266 (2013) 462–470, https://doi.org/10.1148/radiol.12120609.
[43] N. Klein, E. Guenther, F. Botea, M. Pautov, S. Dima, D. Tomescu, M. Popescu, A. Ivorra, M. Stehling, I. Popescu, The combination of electroporation and electrolysis (E2) employing different electrode arrays for ablation of large tissue volumes, PLoS ONE 14 (2019), https://doi.org/10.1371/journal.pone.0221393.
[44] M. Phillips, L. Rubinsky, A. Meir, N. Raju, B. Rubinsky, Combining electrolysis and electroporation for tissue ablation, Technol. Cancer Res. Treat. 14 (2015) 395–410, https://doi.org/10.1177/1533034614560102.
[45] P. Turjanski, N. Olaiz, F. Maglietti, S. Michinski, C. Suárez, F.V. Molina, G. Marshall, The role of pH fronts in reversible electroporation, PLoS ONE 6 (2011), https://doi.org/10.1371/journal.pone.0017303.
[46] N. Olaiz, E. Signori, F. Maglietti, A. Soba, C. Suárez, P. Turjanski, S. Michinski, G. Marshall, Tissue damage modeling in gene electrotransfer: The role of pH, Bioelectrochemistry 100 (2014) 105–111, https://doi.org/10.1016/j.bioelechem.2014.05.001.
[47] F. Maglietti, S. Michinski, N. Olaiz, M. Castro, C. Suárez, G. Marshall, The role of Ph fronts in tissue electroporation based treatments, PLoS ONE 8 (2013), https://doi.org/10.1371/journal.pone.0080167.
[48] J.C. Weaver, K.C. Smith, A.T. Esser, R.S. Son, T.R. Gowrishankar, A brief overview of electroporation pulse strength-duration space: A region where additional intracellular effects are expected, Bioelectrochemistry 87 (2012) 236–243, https://doi.org/10.1016/j.bioelechem.2012.02.007.
[49] C.B. Arena, M.B. Sano, J.H. Rossmeisl, J.L. Caldwell, P.A. Garcia, M.N. Rylander, R. V. Davalos, High-frequency irreversible electroporation (H-FIRE) for non-thermal ablation without muscle contraction, Biomed. Eng. Online 10 (2011), https://doi.org/10.1186/1475-925X-10-102.
[50] M.B. Sano, R.E. Fan, K. Cheng, Y. Saenz, G.A. Sonn, G.L. Hwang, L. Xing, Reduction of Muscle Contractions during Irreversible Electroporation Therapy Using High-Frequency Bursts of Alternating Polarity Pulses: A Laboratory Investigation in an Ex Vivo Swine Model, J. Vasc. Interv. Radiol. 29 (2018) 893–898.e4, https://doi.org/10.1016/j.jvir.2017.12.019.
[51] C. Yao, S. Dong, Y. Zhao, Y. Lv, H. Liu, L. Gong, J. Ma, H. Wang, Y. Sun, Bipolar Microsecond Pulses and Insulated Needle Electrodes for Reducing Muscle Contractions during Irreversible Electroporation, IEEE Trans. Biomed. Eng. 64 (2017) 2924–2937, https://doi.org/10.1109/TBME.2017.2690624.
[52] D.C. Sweeney, M. Reberšek, J. Dermol, L. Rems, D. Miklavčič, R.V. Davalos, Quantification of cell membrane permeability induced by monopolar and high-frequency bipolar bursts of electrical pulses, Biochim. Biophys. Acta - Biomembr. 2016 (1858) 2689–2698, https://doi.org/10.1016/j.bbamem.2016.06.024.
[53] T. Polajžer, J. Dermol-Černe, M. Reberšek, R. O'Connor, D. Miklavčič, Cancellation effect is present in high-frequency reversible and irreversible electroporation, Bioelectrochemistry 132 (2020), https://doi.org/10.1016/j.bioelechem.2019.107442.
[54] M. Scuderi, M. Rebersek, D. Miklavcic, J. Dermol-Cerne, The use of high-frequency short bipolar pulses in cisplatin electrochemotherapy in vitro, Radiol. Oncol. 53 (2019) 194–205, https://doi.org/10.2478/raon-2019-0025.
[55] A. Sugrue, E. Maor, A. Ivorra, V. Vaidya, C. Witt, S. Kapa, S. Asirvatham, Irreversible electroporation for the treatment of cardiac arrhythmias, Expert Rev. Cardiovasc. Ther. 16 (2018) 349–360, https://doi.org/10.1080/14779072.2018.1459185.
[56] D. Miklavčič, G. Pucihar, M. Pavlovec, S. Ribarič, M. Mali, A. MačEk-Lebar, M. Petkovšek, J. Nastran, S. Kranjc, M. Čemažar, G. Serša, The effect of high frequency electric pulses on muscle contractions and antitumor efficiency in vivo for a potential use in clinical electrochemotherapy, Bioelectrochemistry 65 (2005) 121–128, https://doi.org/10.1016/j.bioelechem.2004.07.004.
[57] G. Sersa, S. Kranjc, J. Scancar, M. Krzan, M. Cemazar, Electrochemotherapy of mouse sarcoma tumors using electric pulse trains with repetition frequencies of 1 Hz and 5 kHz, J. Membr. Biol. 236 (2010) 155–162, https://doi.org/10.1007/s00232-010-9268-z.
[58] S. Jaichandran, S.T.B. Yap, A.B.M. Khoo, L.P. Ho, S.L. Tien, O.L. Kon, In vivo liver electroporation: Optimization and demonstration of therapeutic efficacy, Hum. Gene Ther. 17 (2006) 362–375, https://doi.org/10.1089/hum.2006.17.362.
[59] A. Vižintin, J. Vidmar, J. Ščančar, D. Miklavčič, Effect of interphase and interpulse delay in high-frequency irreversible electroporation pulses on cell survival, membrane permeabilization and electrode material release, Bioelectrochemistry 134 (2020), https://doi.org/10.1016/j.bioelechem.2020.107523.
[60] M.B. Sano, C.B. Arena, M.R. DeWitt, D. Saur, R.V. Davalos, In-vitro bipolar nano- and microsecond electro-pulse bursts for irreversible electroporation

therapies, Bioelectrochemistry 100 (2014) 69–79, https://doi.org/10.1016/j.bioelechem.2014.07.010.
[61] R.V. Davalos, B. Rubinsky, L.M. Mir, Theoretical analysis of the thermal effects during in vivo tissue electroporation, Bioelectrochemistry 61 (2003) 99–107, https://doi.org/10.1016/j.bioelechem.2003.07.001.
[62] B.L. Ibey, J.C. Ullery, O.N. Pakhomova, C.C. Roth, I. Semenov, H.T. Beier, M. Tarango, S. Xiao, K.H. Schoenbach, A.G. Pakhomov, Bipolar nanosecond electric pulses are less efficient at electropermeabilization and killing cells than monopolar pulses, Biochem. Biophys. Res. Commun. 443 (2014) 568–573, https://doi.org/10.1016/j.bbrc.2013.12.004.
[63] A.G. Pakhomov, S. Grigoryev, I. Semenov, M. Casciola, C. Jiang, S. Xiao, The second phase of bipolar, nanosecond-range electric pulses determines the electroporation efficiency, Bioelectrochemistry 122 (2018) 123–133, https://doi.org/10.1016/j.bioelechem.2018.03.014.
[64] C.B. Arena, R.V. Davalos, Advances in Therapeutic Electroporation to Mitigate Muscle Contractions, J. Membr. Sci. Technol. 02 (2012), https://doi.org/10.4172/2155-9589.1000e102.
[65] A. Županič, S. Ribarič, D. Miklavčič, Increasing the repetition frequency of electric pulse delivery reduces unpleasant sensations that occur in electrochemotherapy, Neoplasma 54 (2007) 246–250.
[66] M. Wallace, B. Evans, S. Woods, R. Mogg, L. Zhang, A.C. Finnefrock, D. Rabussay, M. Fons, J. Mallee, D. Mehrotra, F. Schödel, L. Musey, Tolerability of two sequential electroporation treatments using MedPulser DNA delivery system (DDS) in healthy adults, Mol. Ther. 17 (2009) 922–928, https://doi.org/10.1038/mt.2009.27.
[67] B. Mercadal, C.B. Arena, R.V. Davalos, A. Ivorra, Avoiding nerve stimulation in irreversible electroporation: A numerical modeling study, Phys. Med. Biol. 62 (2017) 8060–8079, https://doi.org/10.1088/1361-6560/aa8c53.
[68] B. Mali, V. Gorjup, I. Edhemovic, E. Brecelj, M. Cemazar, G. Sersa, B. Strazisar, D. Miklavcic, T. Jarm, Electrochemotherapy of colorectal liver metastases - An observational study of its effects on the electrocardiogram, Biomed. Eng. Online 14 (2015), https://doi.org/10.1186/1475-925X-14-S3-S5.
[69] R. Van Es, M.K. Konings, B.C. Du Pré, K. Neven, H. Van Wessel, V.J.H.M. Van Driel, A.H. Westra, P.A.F. Doevendans, F.H.M. Wittkampf, High-frequency irreversible electroporation for cardiac ablation using an asymmetrical waveform, Biomed. Eng. Online 18 (2019), https://doi.org/10.1186/s12938-019-0693-7.
[70] V.Y. Reddy, P. Neuzil, J.S. Koruth, J. Petru, M. Funosako, H. Cochet, L. Sediva, M. Chovanec, S.R. Dukkipati, P. Jais, Pulsed Field Ablation for Pulmonary Vein Isolation in Atrial Fibrillation, J. Am. Coll. Cardiol. 74 (2019) 315–326, https://doi.org/10.1016/j.jacc.2019.04.021.
[71] B. Howard, D.E. Haines, A. Verma, D. Packer, N. Kirchhof, N. Barka, B. Onal, S. Fraasch, D. Miklavčič, M.T. Stewart, Reduction in Pulmonary Vein Stenosis and Collateral Damage with Pulsed Field Ablation Compared with Radiofrequency Ablation in a Canine Model, Circ. Arrhythmia Electrophysiol. 13 (2020), https://doi.org/10.1161/CIRCEP.120.008337.
[72] W.G. Marshall, B.A. Boone, J.D. Burgos, S.I. Gografe, M.K. Baldwin, M.L. Danielson, M.J. Larson, D.R. Caretto, Y. Cruz, B. Ferraro, L.C. Heller, K.E. Ugen, M.J. Jaroszeski, R. Heller, Electroporation-mediated delivery of a naked DNA plasmid expressing VEGF to the porcine heart enhances protein expression, Gene Ther. 17 (2010) 419–423, https://doi.org/10.1038/gt.2009.153.
[73] A.A. Bulysheva, B. Hargrave, N. Burcus, C.G. Lundberg, L. Murray, R. Heller, Vascular endothelial growth factor-A gene electrotransfer promotes angiogenesis in a porcine model of cardiac ischemia, Gene Ther. 23 (2016) 649–656, https://doi.org/10.1038/gt.2016.35.
[74] S. Dong, C. Yao, Y. Zhao, Y. Lv, H. Liu, Parameters optimization of bipolar high frequency pulses on tissue ablation and inhibiting muscle contraction, IEEE Trans. Dielectr. Electr. Insul. 25 (2018) 207–216, https://doi.org/10.1109/TDEI.2018.006303.
[75] K.N. Aycock, Y. Zhao, M.F. Lorenzo, R.V. Davalos, A theoretical argument for extended interpulse delays in therapeutic high-frequency irreversible electroporation treatments, IEEE Trans. Biomed. Eng. (2021), https://doi.org/10.1109/TBME.2021.3049221.
[76] C. Günter, J. Delbeke, M. Ortiz-Catalan, Safety of long-term electrical peripheral nerve stimulation: Review of the state of the art, J. NeuroEng. Rehabil. 16 (2019), https://doi.org/10.1186/s12984-018-0474-8.
[77] M.B. Sano, C.B. Arena, K.R. Bittleman, M.R. Dewitt, H.J. Cho, C.S. Szot, D. Saur, J. M. Cissell, J. Robertson, Y.W. Lee, R.V. Davalos, Bursts of Bipolar Microsecond Pulses Inhibit Tumor Growth, Sci. Rep. 5 (2015), https://doi.org/10.1038/srep14999.
[78] C. Delteil, J. Teissié, M.P. Rols, Effect of serum on in vitro electrically mediated gene delivery and expression in mammalian cells, Biochim. Biophys. Acta - Biomembr. 1467 (2000) 362–368, https://doi.org/10.1016/S0005-2736(00)00235-2.
[79] M. Bosnjak, B.C. Lorente, Z. Pogacar, V. Makovsek, M. Cemazar, Different incubation times of cells after gene Electrotransfer in fetal bovine serum affect cell viability, but not Transfection efficiency, J. Membr. Biol. 247 (2014) 421–428, https://doi.org/10.1007/s00232-014-9649-9.
[80] M. Golzio, J. Teissié, M.P. Rols, Direct visualization at the single-cell level of electrically mediated gene delivery, Proc. Natl. Acad. Sci. U. S. A. 99 (2002) 1292–1297, https://doi.org/10.1073/pnas.022646499.
[81] S. Haberl, D. Miklavčič, M. Pavlin, Effect of Mg ions on efficiency of gene electrotransfer and on cell electropermeabilization, Bioelectrochemistry 79 (2010) 265–271, https://doi.org/10.1016/j.bioelechem.2010.04.001.
[82] G. Pucihar, J. Krmelj, M. Reberšek, T.B. Napotnik, D. Miklavčič, Equivalent pulse parameters for electroporation, IEEE Trans. Biomed. Eng. 58 (2011) 3279–3288, https://doi.org/10.1109/TBME.2011.2167232.
[83] A. Liew, F.M. André, L.L. Lesueur, M.A. De Ménorval, T. O'Brien, L.M. Mir, Robust, efficient, and practical electrogene transfer method for human mesenchymal stem cells using square electric pulses, Hum. Gene Ther. Methods 24 (2013) 289–297, https://doi.org/10.1089/hgtb.2012.159.
[84] M.-P. Rols, D. Coulet, J. Teissie, Highly efficient transfection of mammalian cells by electric field pulses: Application to large volumes of cell culture by using a flow system, Eur. J. Biochem. 206 (1992) 115–121, https://doi.org/10.1111/j.1432-1033.1992.tb16908.x.
[85] S. Yao, S. Rana, D. Liu, G.E. Wise, Electroporation optimization to deliver plasmid DNA into dental follicle cells, Biotechnol. J. 4 (2009) 1488–1496, https://doi.org/10.1002/biot.200900039.
[86] G. Cheng, J. Zhong, J. Chung, F.V. Chisari, Double-stranded DNA and double-stranded RNA induce a common antiviral signaling pathway in human cells, Proc. Natl. Acad. Sci. U. S. A. 104 (2007) 9035–9040, https://doi.org/10.1073/pnas.0703285104.
[87] K.J. Ishii, T. Kawagoe, S. Koyama, K. Matsui, H. Kumar, T. Kawai, S. Uematsu, O. Takeuchi, F. Takeshita, C. Coban, S. Akira, TANK-binding kinase-1 delineates innate and adaptive immune responses to DNA vaccines, Nature 451 (2008) 725–729, https://doi.org/10.1038/nature06537.
[88] S. Chopra, P. Ruzgys, M. Maciulevičius, M. Jakutavičiute, S. Šatka, Investigation of plasmid DNA delivery and cell viability dynamics for optimal cell electrotransfection in vitro, Appl. Sci. 10 (2020), https://doi.org/10.3390/app10176070.
[89] R.N. Cohen, M.A.E.M. van der Aa, N. Macaraeg, A.P. Lee, F.C. Szoka, Quantification of plasmid DNA copies in the nucleus after lipoplex and polyplex transfection, J. Control. Release 135 (2009) 166–174, https://doi.org/10.1016/j.jconrel.2008.12.016.
[90] Y.C. Tsai, T.H. Tsai, C.P. Chang, S.F. Chen, Y.M. Lee, S.K. Shyue, Linear correlation between average fluorescence intensity of green fluorescent protein and the multiplicity of infection of recombinant adenovirus, J. Biomed. Sci. 22 (2015), https://doi.org/10.1186/s12929-015-0137-z.
[91] S. Haberl, M. Kandušer, K. Flisar, D. Hodžić, V.B. Bregar, D. Miklavčič, J.M. Escoffre, M.P. Rols, M. Pavlin, Effect of different parameters used for in vitro gene electrotransfer on gene expression efficiency, cell viability and visualization of plasmid DNA at the membrane level, J. Gene Med. 15 (2013) 169–181, https://doi.org/10.1002/jgm.2706.
[92] D.E. Chafai, A. Mehle, A. Tilmatine, B. Maouche, D. Miklavčič, Assessment of the electrochemical effects of pulsed electric fields in a biological cell suspension, Bioelectrochemistry 106 (2015) 249–257, https://doi.org/10.1016/j.bioelechem.2015.08.002.
[93] T. Kotnik, D. Miklavčič, L.M. Mir, Cell membrane electropermeabilization by symmetrical bipolar rectangular pulses: Part II. Reduced electrolytic contamination, Bioelectrochemistry (2001) 91–95, https://doi.org/10.1016/S1567-5394(01)00115-3.
[94] T. Potočnik, D. Miklavčič, A. Maček Lebar, Effect of electroporation and recovery medium pH on cell membrane permeabilization, cell survival and gene transfer efficiency in vitro, Bioelectrochemistry 130 (2019), https://doi.org/10.1016/j.bioelechem.2019.107342.
[95] M. Corrotte, T. Castro-Gomes, Lysosomes and plasma membrane repair, Curr. Top. Membr. (2019) 1–16, https://doi.org/10.1016/bs.ctm.2019.08.001.
[96] J.R. Casey, S. Grinstein, J. Orlowski, Sensors and regulators of intracellular pH, Nat. Rev. Mol. Cell Biol. 11 (2010) 50–61, https://doi.org/10.1038/nrm2820.
[97] M. Kandušer, M. Šentjurc, D. Miklavčič, The temperature effect during pulse application on cell membrane fluidity and permeabilization, Bioelectrochemistry 74 (2008) 52–57, https://doi.org/10.1016/j.bioelechem.2008.04.012.
[98] A. Donate, A. Bulysheva, C. Edelblute, D. Jung, M.A. Malik, S. Guo, N. Burcus, K. Schoenbach, R. Heller, Thermal Assisted In Vivo Gene Electrotransfer, Curr. Gene Ther. 16 (2016) 83–89, https://doi.org/10.2174/1566523216666160331125810.
[99] A. Bulysheva, J. Hornef, C. Edelblute, C. Jiang, K. Schoenbach, C. Lundberg, M.A. Malik, R. Heller, Coalesced thermal and electrotransfer mediated delivery of plasmid DNA to the skin, Bioelectrochemistry 125 (2019) 127–133, https://doi.org/10.1016/j.bioelechem.2018.10.004.